Synthesis and Pharmacological Evaluation of a Selected Library of New Potential Anti-inflammatory Agents Bearing the γ-Hydroxybutenolide Scaffold: a New Class of Inhibitors of Prostanoid Production through the Selective Modulation of Microsomal Prostaglandin E Synthase-1 Expression

Maria D. Guerrero,[†] Maurizio Aquino,[‡] Ines Bruno,[‡] María C. Terencio,[†] Miguel Paya,[†] Raffaele Riccio,*[,‡] and Luigi Gomez-Paloma[‡,§]

Dipartimento di Scienze Farmaceutiche, Università degli Studi di Salerno, Via Ponte Don Melillo, 84084 Fisciano (SA), Italy, and Departamento de Farmacología, Facultad de Farmacia, Universidad de Valencia, Avenue Vicente Andrés Estellés s/n, 46100, Burjasot, Valencia, Spain

Received January 22, 2007

As a part of our drug discovery effort, recently we clarified the molecular basis of phospholipase A_2 (PLA_2) inactivation by petrosaspongiolide M (PM), an interesting metabolite belonging to a marine sesterterpene family, containing in its structural architecture a γ-hydroxybutenolide moiety and showing potent anti-inflammatory activity. In the attempt to expand structural diversity as well as to simplify crucial synthetic features of the parent compound, we decided to develop a selected library based on the densely functionalized γ-hydroxybutenolide scaffold. The synthesized products were tested for their ability to inhibit PLA_2 enzymes as well as to modulate the expression of inducible cyclooxygenase 2 (COX-2) and microsomal prostaglandin E synthase 1 (mPGES-1), two key enzymes highly involved in the inflammatory event, in order to discover new promising anti-inflammatory agents with better pharmacological profiles. This led us to the discovery of a promising inhibitor (**4e**) of prostanoid production acting by in vitro and in vivo selective modulation of microsomal prostaglandin E synthase 1 expression.

Introduction

Bioactive natural products can be considered very promising starting points for the development of new therapeutic agents as they are evolutionary selected and basically validated for interfering with biological targets. Hence, libraries designed and synthesized around the basic structure of such compounds have a good chance of displaying biological and pharmacological properties. On the basis of these remarks and continuing our studies on bioactive natural products, we focused our attention on petrosaspongiolides, a family of marine sesterterpenes containing a γ-hydroxybutenolide moiety and displaying a potent anti-inflammatory effect.[1] Of these interesting sponge metabolites, petrosaspongiolide M (PM) (Figure 1) showed a comparatively higher activity mediated by an irreversible inhibition of phospholipase A_2 (PLA_2), the key enzyme involved in the inflammatory response.[2,3] This interesting result prompted us to investigate the molecular mechanism underlying the inactivation of the enzyme and allowed us to propose a model of interaction between the natural ligand and the enzyme active site, in which the γ-hydroxybutenolide moiety seems to play a crucial role.[4] This highly functionalized scaffold can be considered a sort of privileged structure as it is part of the molecular architecture of many marine natural products, such as manoalide,[5] cacospongionolides,[6] dysidiolide,[7] and luffolides[8] (Figure 1), which possess relevant biological activity by virtue of their ability to interact with biological entities. Taking into account these considerations, we decided to generate a focused library of γ-hydroxybutenolide-containing derivatives, with the aim of expanding structural diversity around the natural scaffold and of simplifying the molecular region occupied by the sesterterpene skeleton, likely involved in the molecular recognition process interacting with hydrophobic portion of the enzyme active site. Exploration of the structure−activity relationships of the synthetic products would also provide powerful guiding principles for the development of further generations of analogues and, consequently, for the lead optimization process. For the design of the library we used the Ludi program,[9] which

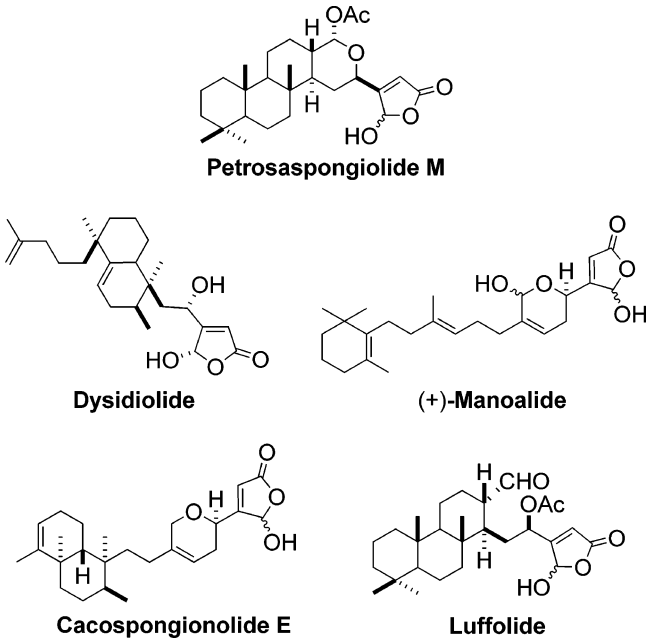

Figure 1. Examples of biologically active natural products bearing a 5-hydroxyfuran-2-one (γ-hydroxybutenolide) moiety.

* Corresponding author: phone +39 089 969 768; fax +39 089 969 602; e-mail riccio@unisa.it.
[†] Universidad de Valencia.
[‡] Università degli Studi di Salerno.
[§] Deceased.

10.1021/jm0700823 CCC: $37.00
Published on Web 04/04/2007

Table 1. Fragments Suggested by LUDI and Their Calculated Scores

entry	structure	LUDI score
1	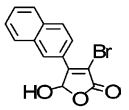	495
2	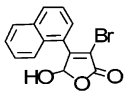	515
3	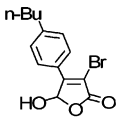	496
4	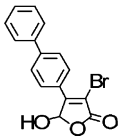	725
5	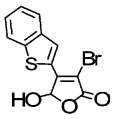	695
6	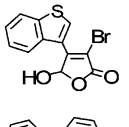	705
7	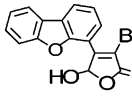	624
8	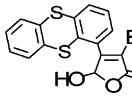	750
9	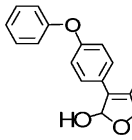	690

was set in order to identify a number of possible fragments, with high binding affinity, in substitution of the sesterterpene skeleton of PM.

In our opinion it is extremely interesting to investigate the putative effects of these derivatives on both $sPLA_2$ activity and on the expression of the inducible enzymes cyclooxygenase 2 (COX-2) and microsomal prostaglandin E synthase 1 (mPGES-1), two key factors involved in the inflammatory response. These effects are correlated with the control on prostaglandin E_2 (PGE_2) production and the involvement of the transcription factor nuclear factor κB (NF-κB).

Results and Discussion

Chemistry. In the preliminary design of the library we decided to insert on the above-mentioned scaffold a series of aromatic and heteroaromatic substituents that presented a high LUDI score (Table 1); in fact, to generate our library we used the 3D structure of the PM−bvPLA_2 complex[4] and the suggestions coming from the LUDI program,[9] a computational method for virtual screening, providing affinity predictions on the basis of a scoring function.

Table 2. Experimental Conditions and Yields

entry	compd	boronic acid equiv	base equiv	time (h)	yield (%)
1	a	2	4	18	82
2	b	2	4	20	89
3	c	2	4	19.5	57
4	d	2	4	18.5	40
5	e	1.5	3	22	62
6	f	1.5	3	23	71
7	g	1.5	3	25	93
8	h	1.5	3	26	42
9	i	1.5	3	22	69

In our case, we used this in silico approach with the intention of generating a series of potential ligands from a known active compound; accordingly, the first step was the removal of the noncovalent binding portion of the lead molecule from the 3D bvPLA_2−PM model, consisting exactly of the sesterterpene skeleton[4] holding the γ-hydroxybutenolide pharmacophore. Then a number of possible fragments were selected by the software to build potential ligands with putative high-affinity binding for the target enzyme. Going to the executive plane of the project, we estimated that the more feasible route to generate these compounds was to start from an appropriately protected γ-hydroxybutenolide moiety, which would be decorated with the selected substituents through an organometallic-catalyzed cross-coupling reaction. Consequently, the synthesis can be divided into three main steps: (a) generation of the starting building block, (b) coupling reaction, and (c) deprotection of the coupling adduct (Scheme 1).

Accordingly we considered, as a simple access to the butenolide moiety, the use of the commercially available mucobromic acid **1**,[10] containing a vinyl dibromide function that can act as electrophilic partner in a Pd-catalyzed cross-coupling reaction.[11] We selected as hydroxyl protecting group of hemiacetal function the base-stable methoxyethoxymethoxy (Mem) group,[12] which is perfectly compatible with the conditions of the following Suzuki coupling process. To achieve the best experimental conditions, we utilized as a model reaction the coupling of **2** with 2-naphthaleneboronic acid (Scheme 1), and taking advantage of these preliminary trials, we obtained the desired protected product in good yield, with low formation of byproducts, mainly consisting of bis-coupling and homocoupling adducts. Finally, removal of the Mem protecting group, by use of $AlCl_3$ in CH_2Cl_2, afforded compound **4a**. In order to verify whether such experimental conditions could also be applied to heteroaromatic moieties, with an expected different reactivity, we performed the reaction on 3-benzothiopheneboronic acid (**4f**). The obtained results allowed us to refine reaction conditions on heteroaromatic substrates (Table 2).

The next stage was to perform the Suzuki coupling on all the selected boronic acids (Table 2). To this end, we followed a parallel protocol by using the ASW1000 Chemspeed apparatus, which allowed us to obtain compounds **4a**−**i** with a single programmed process (Chart 1).

It is worth noting that the synthetic procedure provided, in all cases, satisfactory yields of the desired monosubstituted γ-hydroxybutenolide analogues, with lower amounts of bis-substituted adducts as major byproducts. We decided to select compound **5** (Chart 1), the byproduct of **4a**, in order to evaluate the impact on the biological activity of an additional hydrophobic substituent on the pharmacophoric core.

Biology. Marine organisms, especially sponges, are a rich source of molecules exhibiting PLA_2 inhibitory properties in vitro and in vivo, mainly on secretory enzymes, compared to cytosolic ones ($cPLA_2$).[13] Type IIA $sPLA_2$, the best-studied

Scheme 1. Synthesis of PM Analogues **4a**−**i**[a]

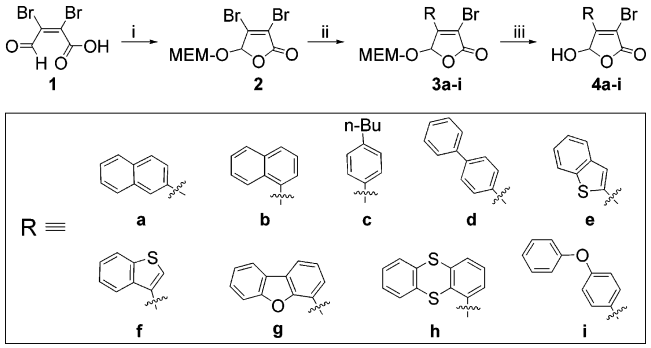

[a] Reagents and conditions: (i) MEM-Cl, DIPEA, CH_2Cl_2, rt, 4 h, 86%; (ii) $PdCl_2(PPh_3)_2$, R-$B(OH)_2$, $BnEt_3N^+Cl^-$, CsF, toluene, H_2O, 60 °C; (iii) $AlCl_3$, CH_2Cl_2, 0 °C, 4 h, quant.

Chart 1. Collection of PM analogues

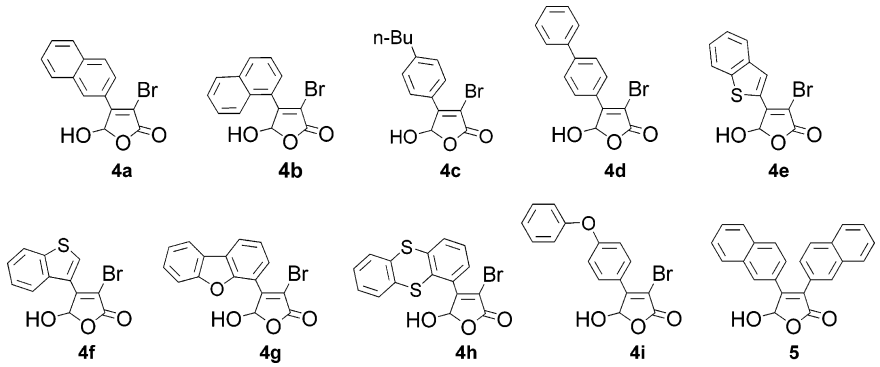

enzyme of $sPLA_2$, has been detected at high levels in various inflamed sites, suggesting its involvement in pathogenesis of the inflammatory responses.

Moreover, the enzyme concentration in serum tissues correlates with disease severity in several immune-mediated inflammatory pathologies, such as rheumatoid arthritis, septic shock, psoriasis, Crohn's disease, and asthma.[14−17] Group IIA $sPLA_2$ has been reported to release arachidonic acid in many systems and to provide the substrate for both cyclooxygenase (COX) and 5-lipoxygenase (5-LO) derivatives.[18] Prostaglandin E_2 (PGE_2) contributes to the pathogenesis of different inflammatory diseases, acting as a mediator of pain and inflammation and promoting bone destruction. Therefore, regulation of the synthesis or action of PGE_2 has important therapeutical implications. COX and prostaglandin E synthase (PGES) are inducible enzymes responsible for PGE_2 synthesis.[19] Of the bioactive marine natural products, petrosaspongiolide M (PM), a potent inhibitor of $sPLA_2$ with anti-inflammatory properties in several experimental models, is able to reduce cytokine, nitric oxide, and PGE_2 production through the inhibition of iNOS and COX-2 expression via NF-κB pathway.

The 10 new γ-hydroxybutenolide derivatives have been tested at 10 μM (Table 3) under the same experimental conditions on four different $sPLA_2$ belonging to groups IA (*Naja naja* venom), IB (porcine pancreatic enzyme), IIA (human synovial recombinant), and III (bee venom enzyme). Of the γ-hydroxybutenolide derivatives, only compound **4c** preferentially inhibited human synovial $sPLA_2$, with an inhibition percentage close to 50%, showing lower potency toward this enzyme than those of the reference inhibitors, PM and LY311727.

The effect of the γ-hydroxybutenolide derivatives on PGE_2 production on mouse macrophage cell line RAW264.7 stimulated with LPS was determined (Figure 2). After 18 h of stimulation, compound **4e** was the only one able to inhibit PGE_2 production with a percentage of inhibition higher than 50% at 10 μM, showing an IC_{50} value of 1.8 μM (0.5−3.8 interval of confidence) (Figure 3).

Table 3. Inhibitory Activity of the γ-Hydroxybutenolide Derivatives at 10 μM on Different $sPLA_2$[a,b]

compd (10 μM)	group IA $sPLA_2$, % I	group IB $sPLA_2$, % I	group IIA $sPLA_2$, % I	group III $sPLA_2$, % I
4a	9.2 ± 1.1	27.7 ± 7.9	19.4 ± 2.6**	14.7 ± 2.3
4b	8.6 ± 2.4	13.7 ± 8.3	5.3 ± 3.8	0.0 ± 0.0
4c	26.0 ± 2.3	35.1 ± 10.0	50.9 ± 5.8**	32.9 ± 3.5*
4d	7.5 ± 1.5	26.0 ± 13.6	33.2 ± 2.3**	14.4 ± 2.2
4e	3.4 ± 1.5	18.7 ± 8.4	5.1 ± 1.9	0.0 ± 0.0
4f	15.4 ± 2.9	33.5 ± 8.5	24.4 ± 3.4**	9.8 ± 6.2
4g	0.0 ± 2.1	38.6 ± 4.9	23.5 ± 3.0**	20.4 ± 1.4
4h	1.5 ± 1.1	0.0 ± 0.0	0.8 ± 0.8	0.0 ± 0.0
4i	1.0 ± 1.0	7.8 ± 1.5	33.7 ± 1.8**	2.1 ± 1.7
5	9.1 ± 9.1	22.5 ± 10.5	26.0 ± 2.6**	25.2 ± 10.4
PM	5.4 ± 2.1	11.4 ± 4.6	79.4 ± 3.6**	60.8 ± 5.3**
LY	2.7 ± 2.7	6.8 ± 6.8	90.5 ± 1.6**	0.0 ± 0.0

[a] Different $sPLA_2$: groups IA (*Naja naja* venom), IB (porcine pancreatic enzyme), IIA (human synovial recombinant), and III (bee venom enzyme). [b] Results show mean ± SEM ($n = 6$). Statistical significance: ** $p < 0.01$, * $p < 0.05$.

On the other hand, compounds **4a**−**i** and **5** were devoid of significant cytotoxic effects on RAW264.7 at concentrations up to 10 μM, as assessed by the mitochondrial-dependent reduction of 3-(4,5-dimethylthiazol-2-yl)-2,5-diphenyltetrazolium bromide (MTT) to formazan (data not shown). To establish whether the inhibition of PGE_2 production was due to an interaction with the enzyme induction by LPS or to a direct inhibitory action on COX-2 and mPGES-1 enzymatic activities, compound **4e** was added to cells that previously had expressed COX-2 and mPGES-1 and was then incubated for 2 h in fresh culture medium supplemented with arachidonic acid (Table 4).

Compound **4e**, which caused a significant reduction in PGE_2 production in the induction phase, did not affect PGE_2 produc-

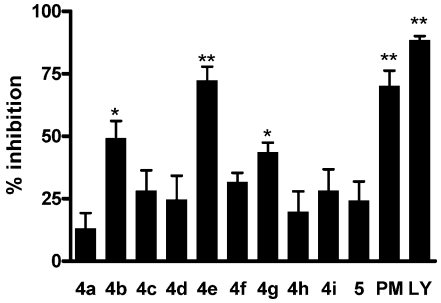

Figure 2. Inhibitory activity of the γ-hydroxybutenolide derivatives at 10 μM on the production of PGE_2 in LPS-stimulated RAW264.7 cells. Statistical significance: $^{**}p < 0.01$, $^{*}p < 0.05$.

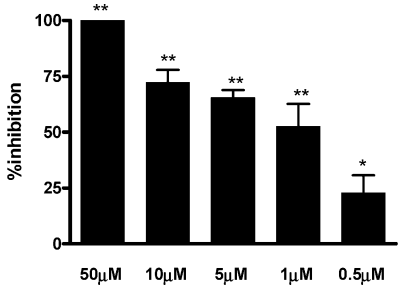

Figure 3. Dose-dependent inhibitory effect of γ-hydroxybutenolide **4e** on the production of PGE_2 in LPS-stimulated RAW264.7 cells. Statistical significance: $^{**}p < 0.01$, $^{*}p < 0.05$.

Table 4. Inhibitory Activity of γ-Hydroxybutenolide Derivative **4e** on the Production of PGE_2 in LPS-Stimulated RAW264.7 Cells[a]

	PGE_2 production (ng/mL)	
	18 h treatment (induction phase)	2 h treatment (postinduction phase)
nonstimulated cells	1.6 ± 0.2**	0.06 ± 0.01**
LPS-stimulated cells	20.7 ± 2.0	0.22 ± 0.01
4e, 10 μM	6.7 ± 1.1**	0.22 ± 0.01
4e, 1 μM	10.7 ± 1.9**	0.23 ± 0.01
dexamethasone, 1 μM	3.4 ± 1.1**	0.21 ± 0.02
NS398, 10 μM	ND	0.07 ± 0.01**
PM, 1 μM	7.3 ± 1.2 **	0.22 ± 0.01

[a] Results show mean $\pm$ SEM ($n = 6$). ND, not determined. Statistical significance: $^{**}p < 0.01$ compared with LPS-stimulated cells.

tion content in the postinduction phase, whereas the selective inducible COX-2 inhibitor NS398 caused a marked inhibition of PGE_2 production. In addition, dexamethasone, an inhibitor of inducible COX-2 and mPGES-1, significantly modified the level of this metabolite only in the induction phase. This suggests that compound **4e** could play an inhibitory profile, acting as an inducible COX-2 and/or mPGES-1 expression inhibitor.

Western blot analysis for COX-2 and mPGES-1 proteins with 18 h LPS-stimulated RAW 264.7 cells (Figure 4A) shows clearly that compound **4e** inhibits dose-dependently mPGES-1 expression, without any effect on COX-2 expression, whereas dexamethasone, as expected, reduced the expression of both inducible proteins. With regard to 18 h LPS-stimulated THP-1 cells (Figure 4B), very similar results are shown for mPGES-1. COX-2 expression is just slightly inhibited by compound **4e** (at 10 μM), but not at all at 1 μM concentration. Dexamethasone, as shown, reduced the expression of both inducible proteins (COX-2 and mPGES-1) for THP-1 cells.

We also evaluated the in vivo pharmacological profile of compound **4e** in the 24 h zymosan-stimulated mouse air pouch model of inflammation (Figure 5). At this time point, a high expression of COX-2 and mPGES-1 protein was detected by Western blotting in the cells accumulating in the air pouch exudates; whereas compound **4e** administration selectively decreased the expression of mPGES-1, dexamethasone inhibited the expression of both inducible proteins.

To evaluate the role of NF-κB in the mechanism of action of compound **4e**, we analyzed nuclear protein extracts from mouse macrophage cell line RAW264.7, stimulated with LPS either in the presence or absence of compound **4e**, for NF-κB-DNA binding activity using a radiolabeled NF-κB-specific oligonucleotide (Figure 6). Strong radioactive DNA binding to nuclear proteins was observed after 1 h when cells were treated with LPS. Nuclear extracts of cells incubated with compound **4e** and LPS showed a protein−DNA complex migrating at the same mobility, which was reduced dose-dependently, as compared to the LPS control at concentrations of 1 and 10 μM. The proteasome inhibitor MG132 and PM, used as reference compounds, inhibited NF-κB−DNA binding activity. The $sPLA_2$ inhibitor LY311727 did not affect this transcriptional nuclear factor. Our data demonstrate that compound **4e** is at least a potent inhibitor of NF-κB−DNA binding activity. Whether this compound interferes with the IkB kinase complex or upstream kinases such as NF-κB-inducing kinase and mitogen-activated protein kinase (MAPK)/ERK kinase−kinase-1[20] or could interfere in addition with other transcription factors such as peroxisome proliferator-activated receptors (PPARs)[21] or Egr-1[22] remains to be elucidated.

PGE_2 is by far the major prostanoid synthesized in the joint and plays an important role in different inflammatory diseases, acting as a mediator of pain and inflammation and promoting bone destruction.[23] PGE_2 is generated at sites of inflammation in substantial amounts and can mediate many of the pathologic features of inflammation.[24] To affect this wide terrain of cellular responses, PGE_2 interacts with specific receptors, termed EP1−4, that have a restricted patterns of expression and receptor-specific actions.[25] Therefore, regulation of the synthesis or action of PGE_2 has important therapeutical implications.[26] In this regard, there are at least three approaches to control PGE_2 production:[27] enzymatic inhibitors of $sPLA_2$, which in theory limit arachidonic acid availability; nonsteroidal antiinflammatory drugs (NSAIDs), which inhibit enzymatically COX1−2 isoforms; and glucocorticoids, which inhibit the expression of a great number of proinflammatory proteins such as COX-2, mPGES-1, and iNOS. Each of these three reactions can be rate-limiting and involves multiple enzymes/isozymes that can act in different phases of cell activation and exhibit distinct functional coupling.[28]

Since conventional NSAIDs inhibit COX-2 and also affect physiological prostanoid production due to COX-1 inhibition, it is of great interest to selectively modulate COX-2.[29] In addition, COX and prostaglandin E synthase (PGES) are the main inducible enzymes responsible for PGE_2 synthesis,[30] and both of them are downregulated by glucocorticoids in various cells.[31,32] Recently, it has been shown that synoviocytes isolated from patients with rheumatoid arthritis coexpress both mPGES-1 and COX-2 and generate high amounts of PGE_2 after treatment with proinflammatory cytokines.[33] The evaluation of the effects of antirheumatic treatments on the PGE_2 biosynthetic pathway suggest that the inhibition of PGE_2 biosynthesis, preferably by targeting mPGES-1, might complement anti-TNF treatment for optimal anti-inflammatory results in rheumatoid arthritis.[34]

Conclusions

In this work we elaborated a suitable strategy to simplify the access to a collection of compounds containing the γ-hydroxybutenolide scaffold, through a typical parallel synthetic approach.

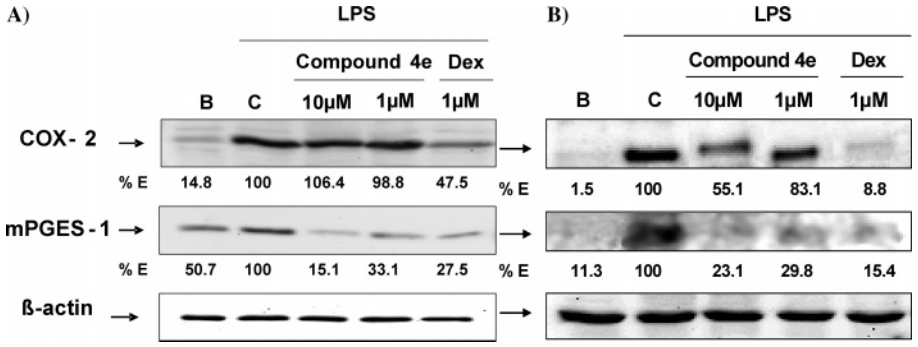

Figure 4. Effect of γ-hydroxybutenolide **4e** on COX-2 and mPGES-1 expression in LPS-stimulated RAW264.7 cells (A) and THP-1 (B). Densitometric analysis is expressed as percentage of maximal band intensity (LPS control group). The figures are representative of two similar experiments. B, normal cells; C, LPS-stimulated cells; Dex, dexamethasone.

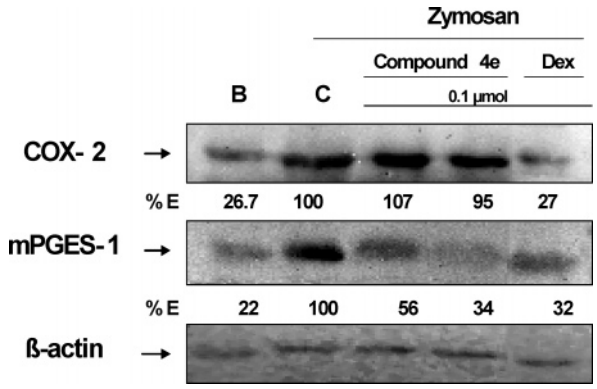

Figure 5. In vivo effect of γ-hydroxybutenolide **4e** on COX-2 and mPGES-1 expression in 24 h zymosan-stimulated mouse air pouch. Densitometric analysis is expressed as percentage of maximal band intensity (zymosan control group). The figure is representative of two similar experiments. B, normal cells; C, zymosan-stimulated cells; Dex, dexamethasone.

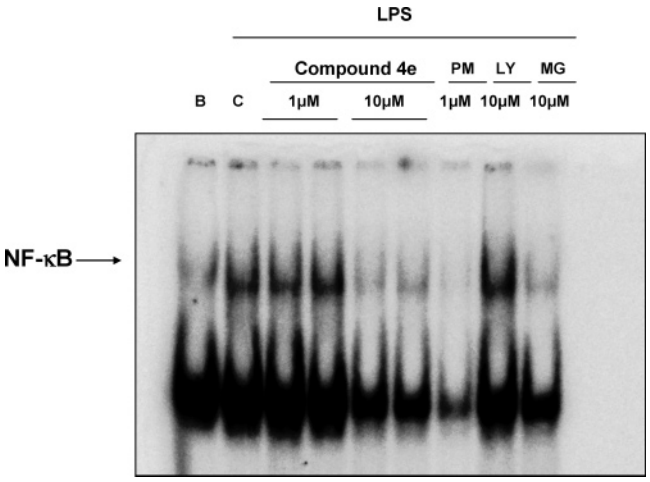

Figure 6. Effect of γ-hydroxybutenolide **4e** on NF-κB-DNA binding activity in nuclear extracts of LPS-stimulated RAW264.7 cells. The figure is representative of two independent experiments. B, normal cells; C, LPS-stimulated cells.

Furthermore, all the synthesized compounds were subjected to pharmacological screening in order to test their inhibitory activity toward different $sPLA_2$ and on the production of PGE_2. Our data demonstrate that compound **4e** is a potent inhibitor of PGE_2 production through the selective modulation of mPGES-1 without affecting COX-2 expression in murine macrophage RAW 264.7 as well as in human monocytic THP-1 cell lines. The COX-2 and mPGES-1 expression profile for compound **4e** was confirmed in the air pouch model of inflammation. In this respect, the use of drugs possessing distinct mechanisms of actions may be of relevance and could be an important strategy to obtain promising anti-inflammatory agents, as well as to provide a pharmacological tool to discern the role of mPGES-1 and COX-2 in a great number of inflammatory disorders.

Experimental Section

LUDI Design. The Ludi module of Insight II (Accelrys, San Diego, CA) was used for the in silico design. Computation was performed on a Silicon Graphics Indigo 2 workstation equipped with a R10000 processor. The 3D complex structure $bvPLA_2$ (1POC)-PM[4] was imported into the graphic modeling program Insight II; the tetracyclic portion of PM was deleted from the active site of the above-mentioned adduct, whereas the tridimensional coordinates of the γ-hydroxybutenolide ring were kept unaltered. On this data set, LUDI performed a database screening on the User_link_library (provided by Accelerys version 1998 and 2000.2) to select appropriate aromatic and heteroaromatic fragments to replace the sesterterpene skeleton of PM by linking the γ-hydroxybutenolide ring. The value of the maximum RMS deviation was fixed at 0.4 Å, the lipo weight was set at 10, the H bond weight was set at 1, and the value of the minimum separation was definitively 3.00. The other parameters were used as standard default. For each fragment, the LUDI score was calculated by means of the scoring function mentioned as *energy estimate_3*.

General Methods. All water- and air-sensitive reactions were carried out under an inert atmosphere (N_2) in oven- or flame-dried glassware. Methylene chloride and toluene were distilled from CaH_2 immediately prior to use. Water was degassed under vacuum (10 mbar). All reagents were used from commercial sources without any further purification. Organic extracts were dried over anhydrous Na_2SO_4. Reactions were monitored on silica gel 60 F254 (Merck) plates and visualized with potassium permanganate or cerium sulfate under UV (λ = 254, 365 nm). Flash column chromatography was performed by use of Merck 60/230−400 mesh silica gel. Analytical and semipreparative reverse-phase HPLC purifications were performed on a Waters instrument with a Jupiter C-18 column (250 × 4.60 mm, 5 μm, 300 Å; and 250 × 10.00 mm, 10 μm, 300 Å, respectively). Purity grade of final products was determined on a Agilent 1100 HPLC with two different analytical reverse-phase columns (method A, Jupiter C-18, 250 × 4.60 mm, 5 μm, 300 Å; method B, Jupiter C-4, 250 × 4.60 mm, 5 μm, 300 Å). Parallel reactions were performed on a Chemspeed automated synthesis workstation ASW1000. Reaction yields refer to chromatographically and spectroscopically pure products. Proton-detected [^{1}H, heteronuclear multiple bond correlation (HMBC), and heteronuclear single quantum coherence (HSQC)] and carbon-detected NMR spectra were recorded on Bruker instruments of Avance series operating at 300, 400, and 600 MHz and at 75, 100, and 150 MHz, respectively. Chemical shifts are expressed in parts per million (ppm) on the delta (δ) scale. The solvent peak was used as internal reference: for ^{1}H NMR, $CDCl_3$ = 7.25 ppm; for ^{13}C NMR, $CDCl_3$ = 77.0 ppm. Multiplicities are reported as follows: (s = singlet; d

= doublet; t = triplet; q = quartet; quint = quintet; sext = sextet; dd = doublet of doublets; dt = doublet of triplets; br = broad). High-resolution mass spectra were recorded on a Q/TOF Premier Waters (Milford, MA) mass spectrometer by use of an electrospray ion source (ESI-MS).

3,4-Dibromo-5-[(2-methoxyethoxy)methoxy]-5*H*-furan-2-one (2). To a solution of mucobromic acid (**1**) (100 mg, 0.387 mmol) in 10 mL of dry dichloromethane was added MEM-Cl (66 μL, 0.581 mmol). Diisopropylethylamine (101 μL, 0.581 mmol) was added dropwise over a period of 15 min. After 4 h, the reaction was quenched with 20 mL of 1 M HCl. The aqueous layer was extracted with dichloromethane (2 × 30 mL) and the organics were dried, filtered, and concentrated in vacuo to leave a dark oil. The crude oil was purified by flash chromatography (10% diethyl ether/hexane) to give **2** (115 mg, 86% yield): ^{1}H NMR (300 MHz; $CDCl_3$) δ 3.40 (3H, s, OC*H*$_3$), 3.54 (2H, dd, OCH$_2$C*H*$_2$O), 3.60 (1H, m, OCH*H*CH$_2$O), 3.79 (1H, m, OC*H*HCH$_2$O), 4.87 (1H, d, J = 7 Hz, OCH*H*O), 5.20 (1H, d, J = 7 Hz, OC*H*HO), 6.10 (1H, s, *H*-5); ^{13}C NMR (75 MHz; $CDCl_3$) δ 59.8, 69.0, 72.1, 95.2, 100.4, 119.1, 144.2, 167.4; HRMS calcd for $C_8H_{11}Br_2O_5$ [M + H]$^+$ 344.8973, 346.8953, 348.8932 (ratio 1:2:1); found [M + H]$^+$ 344.8942, 346.8925, 348.8918 (ratio 1:2:1).

General Procedure for Suzuki Coupling of 2. In a two-neck flask, compound **2** (200 mg, 0.578 mmol) in 3 mL of a degassed mixture of toluene/water (2:1) was dissolved under a N_2 atmosphere. Upon stirring, the desired boronic acid (1.5 or 2 equiv, see Table 2), $PdCl_2(PPh_3)_2$ (20.3 mg, 0.0289 mmol), and benzyltriethylammonium chloride (6.6 mg, 0.0289 mmol) were added. CsF (3 or 4 equiv, see Table 2), first dissolved in 1 mL of degassed water, was finally introduced into the solution. The mixture was then warmed to 60 °C and stirred under N_2 until the reaction appeared complete by TLC (16−20 h depending on the boronic acid; see Table 2). The solution was then diluted with 20 mL of toluene and washed with 1 N HCl aqueous solution (20 mL). The aqueous layer was re-extracted (2 × 30 mL) and the organics were dried, filtered, and concentrated in vacuo. The brown oil was purified by flash chromatography (10% diethyl ether/hexane) to give, depending on the starting material, compounds **3a**−**i**.

General Procedure for Deprotection of Compounds 3a−i. A solution of $AlCl_3$ (5 equiv) in 2 mL of dry dichloromethane was cooled to 0 °C and, upon stirring, a solution of **3a**−**i** in 1 mL of dry dichloromethane was slowly added. After 4 h, the reaction was quenched with saturated $NaHCO_3$ (5 mL) and extracted with CH_2Cl_2 (3 × 10 mL). The organics were then washed with brine, dried, filtered, and concentrated in vacuo, to leave a yellow oil that was purified on a C-18 RP-HPLC column, leaving the desired product (**4a**−**i**) as a solid.

3-Bromo-5-hydroxy-4-naphthalen-2-yl-5*H*-furan-2-one (4a). ^{1}H NMR (300 MHz, MeOD) δ 6.72 (1H, s, OC*H*OH), 7.60 (2H, m, *H*-7, *H*-6), 7.93 (1H, d, J = 8.8 Hz, *H*-5), 7.99 (2H, m, *H*-4, *H*-3), 8.10 (1H, dd, J = 1.8, 8.7 Hz, *H*-8), 8.54 (1H, br s, *H*-1); ^{13}C NMR (75 MHz, D_2O) δ 97.8, 109.8, 123.8, 125.4, 126.3, 126.9, 127.7, 128.5, 128.9, 129.4, 132.4, 134.2, 155.0, 166.4; HRMS calcd for $C_{14}H_8BrO_3$ [M − H]$^-$ 302.9657 and 304.9636 (ratio 1:1), found 302.9682 and 304.9671 (ratio 1:1).

3-Bromo-5-hydroxy-4-naphthalen-1-yl-5*H*-furan-2-one (4b). ^{1}H NMR (300 MHz, $CDCl_3$) δ 6.51 (1H, s, OC*H*OH), 7.52 (1H, dd, J = 1.4, 7.1 Hz, *H*-8), 7.59 (3H, m, *H*-3, *H*-6, *H*-7), 7.71 (1H, dd, J = 3.4, 6.3 Hz, *H*-5), 7.94 (1H, dd, J = 3.3, 6.3 Hz, *H*-4), 7.99 (1H, d, *H*-2); ^{13}C NMR (75 MHz, $CDCl_3$) δ 97.8, 116.6, 125.4, 125.7, 126.7, 127.3, 127.6, 127.9, 129.5, 130.0, 131.5, 134.2, 160.0, 167.0; HRMS calcd for $C_{14}H_8BrO_3$ [M − H]$^-$ 302.9657 and 304.9636 (ratio 1:1), found 302.9674 and 304.9690 (ratio 1:1).

3-Bromo-4-(4-butylphenyl)-5-hydroxy-5*H*-furan-2-one (4c). ^{1}H NMR (300 MHz, $CDCl_3$) δ 0.94 (3H, t, J = 7.3 Hz, C*H*$_3$), 1.37 (2H, sext, J = 7.7, 14.5 Hz, C*H*$_2$), 1.63 (2H, quint, J = 7.7, 15.3 Hz, C*H*$_2$), 2.67 (2H, t, J = 7.7 Hz, C*H*$_2$), 6.51 (1H, s, OC*H*OH), 7.33 (2H, t, J = 8.2 Hz, *H*-3, *H*-5), 7.94 (2H, t, J = 8.2 Hz, *H*-2, *H*-6); ^{13}C NMR (75 MHz, $CDCl_3$) δ 13.7, 22.1, 33.1, 35.2, 97.8, 109.2, 125.9, 127.8, 127.9, 128.6, 128.7, 147.0, 153.9, 166.3; HRMS calcd for $C_{14}H_{14}BrO_3$ [M − H]$^-$ 309.0126 and 311.0106 (ratio 1:1), found 309.0112 and 311.0131 (ratio 1:1).

4-Biphenyl-4-yl-3-bromo-5-hydroxy-5*H*-furan-2-one (4d). ^{1}H NMR (300 MHz, D_2O) δ 6.55 (1H, s, OC*H*OH), 7.39 (1H, t, *H*-10), 7.48 (2H, t, J = 6.4 Hz, *H*-9, *H*-11), 7.64 (2H, d, J = 6.6 Hz, *H*-8, *H*-12), 7.75 (2H, d, J = 8.4 Hz, *H*-3, *H*-5), 8.11 (2H, d, J = 8.3 Hz, *H*-2, *H*-6); ^{13}C NMR (150 MHz, $CDCl_3$) δ 98.6, 108.6, 117.6, 120.4, 120.5, 123.2, 125.2, 130.6, 130.7, 130.8, 130.8, 130.9, 154.3, 155.2, 161.1, 166.8; HRMS calcd for $C_{16}H_{10}BrO_3$ [M − H]$^-$ 328.9813 and 330.9793 (ratio 1:1), found 328.9844 and 330.9815 (ratio 1:1).

4-Benzo[*b*]thiophen-2-yl-3-bromo-5-hydroxy-5*H*-furan-2-one (4e). ^{1}H NMR (300 MHz, $CDCl_3$) δ 6.54 (1H, s, OC*H*OH), 7.46 (2H, m, *H*-6, *H*-7), 7.95 (2H, d, *H*-5, *H*-8), 8.15 (1H, s, *H*-3); ^{13}C NMR (75 MHz, $CDCl_3$) δ 98.75, 112.90, 123.6, 124.0, 125.2, 125.6, 130.0, 135.7, 136.2, 140.5, 150.2, 166.7; HRMS calcd for $C_{12}H_6BrO_3S$ [M − H]$^-$ 308.9221 and 310.9201 (ratio 1:1), found 308.9250 and 310.9227 (ratio 1:1).

4-Benzo[*b*]thiophen-3-yl-3-bromo-5-hydroxy-5*H*-furan-2-one (4f). ^{1}H NMR (300 MHz, D_2O) δ 6.62 (1H, s, OC*H*OH), 7.50 (2H, m, *H*-6, *H*-7), 7.87 (1H, d, *H*-5), 7.97 (1H, d, *H*-8), 8.18 (1H, s, *H*-2); ^{13}C NMR (75 MHz, D_2O) δ 99.1, 112.9, 123.6, 124.0, 125.2, 125.6, 130.0, 131.4, 136.2, 140.5, 153.8, 166.7; HRMS calcd for $C_{12}H_6BrO_3S$ [M − H]$^-$ 308.9221 and 310.9201 (ratio 1:1), found 308.9248 and 310.9224 (ratio 1:1).

3-Bromo-4-dibenzofuran-4-yl-5-hydroxy-5*H*-furan-2-one (4g). ^{1}H NMR (300 MHz, $CDCl_3$) δ 6.77 (1H, s, OC*H*OH), 7.46 (1H, t, J = 7.7 Hz, *H*-7), 7.47 (1H, t, J = 7.7 Hz, *H*-8), 7.60 (1H, t, J = 8.3 Hz, *H*-2), 7.70 (1H, d, J = 8.2 Hz, *H*-3), 7.85 (1H, d, J = 8.3 Hz, *H*-1), 8.04 (1H, d, J = 7.7 Hz, *H*-6), 8.14 (1H, d, J = 7.7 Hz, *H*-9); ^{13}C NMR (75 MHz, $CDCl_3$) δ 97.8, 109.8, 123.8, 125.4, 125.5, 126.3, 126.9, 127.7, 128.5, 128.6, 128.9, 132.4, 134.2, 149.8, 155.0, 166.3; HRMS calcd for $C_{16}H_8BrO_4$ [M − H]$^-$ 342.9606 and 344.9585 (ratio 1:1), found 342.9639 and 344.9565 (ratio 1:1).

3-Bromo-5-hydroxy-4-thianthren-1-yl-5*H*-furan-2-one (4h). ^{1}H NMR (600 MHz, $CDCl_3$) δ 6.62 (1H, s, OC*H*OH), 7.27 (1H, m, *H*-7, *H*-8, *H*-1), 7.35 (1H, t, *H*-2), 7.45 (1H, d, *H*-9), 7.53 (1H, d, *H*-6), 7.55 (1H, d, *H*-3); ^{13}C NMR (150 MHz, $CDCl_3$) δ 100.2, 116.8, 128.0, 128.3, 128.6, 128.9, 129.2, 129.7, 130.4, 130.9, 131.9, 134.6, 136.1, 137.9, 156.0, 166.3; HRMS calcd for $C_{16}H_8BrO_3S_2$ [M − H]$^-$ 390.9098 and 392.9078 (ratio 1:1), found 390.9115 and 392.9102 (ratio 1:1).

3-Bromo-5-hydroxy-4-(4-phenoxyphenyl)-5*H*-furan-2-one (4i). ^{1}H NMR (300 MHz, D_2O) δ 6.52 (1H, s, OC*H*OH), 7.10 (2H, d, *H*-12, *H*-8), 7.12 (2H, d, J = 7.4 Hz, *H*-3, *H*-5), 7.24 (1H, t, J = 7.4 Hz, *H*-10), 7.43 (2H, t, J = 7.4 Hz, *H*-11, *H*-9), 8.05 (2H, d, J = 8.8 Hz, *H*-2, *H*-6); ^{13}C NMR (75 MHz, D_2O) δ 98.1, 108.6, 117.6, 117.7, 120.4, 120.5, 123.2, 125.2, 130.6, 130.7, 130.8, 130.9, 154.3, 155.3, 161.1, 166.8; HRMS calcd for $C_{16}H_{10}BrO_4$ [M − H]$^-$ 344.9762 and 346.9742 (ratio 1:1), found 344.9791 and 346.9755 (ratio 1:1).

5-Hydroxy-3,4-dinaphthalen-2-yl-5*H*-furan-2-one (5). ^{1}H NMR (300 MHz, $CDCl_3$) δ 6.74 (1H, s, OC*H*OH), 7.38 (2H, d, J = 4.3 Hz, *H*-8′, *H*-5′), 7.45 (4H, m, *H*-7, *H*-6, *H*-7′, *H*-6′), 7.70 (1H, d, *H*-5), 7.80 (4H, d, *H*-4, *H*-3, *H*-4′, *H*-3′), 7.85 (1H, d, *H*-8), 8.05 (1H, s, *H*-1′), 8.13 (1H, s, *H*-1); ^{13}C NMR (75 MHz, D_2O) δ 97.8, 109.8, 123.6, 123.8, 125.4, 125.8, 126.3, 126.4, 126.9, 127.1, 127.2, 127.7, 128.2, 128.5, 128.6, 128.9, 129.4, 130.2, 132.4, 132.8, 134.2, 135.0, 144.0, 166.4; HRMS calcd for $C_{24}H_{15}O_3$ [M − H]$^-$ 351.1021, found 351.1007.

Materials. [5,6,8,11,12,14,15(*n*)-^{3}H]PGE$_2$ and [9,10-^{3}H$_2$]oleic acid were purchased from Amersham Biosciences (Barcelona, Spain). LY311727 was a gift from Lilly Corporate Center (Indianapolis, IN). The rest of the reagents were from Sigma (St. Louis, MO). *Escherichia coli* strain CECT 101 was a gift from Professor Uruburu, Department of Microbiology, University of Valencia, Spain.

Assay of sPLA$_2$. sPLA$_2$ activity was assayed by use of [^{3}H]-oleate-labeled membranes of *E. coli*, following a modification of the method of Franson and co-workers[35,36] *E. coli* strain CECT 101 was grown for 6−8 h at 37 °C in the presence of 5 μCi/mL [^{3}H]-

oleic acid (specific activity 10 Ci/mmol) until the end of the logarithmic phase. After centrifugation at 1800*g* for 10 min at 4 °C, the membranes were washed, resuspended in phosphate-buffered saline (PBS) and autoclaved for 30−45 min. At least 95% of the radioactivity was incorporated into the phospholipid fraction. *Naja naja* venom (group IA $sPLA_2$), porcine pancreatic (group IB $sPLA_2$), human recombinant synovial (group IIA $sPLA_2$), and bee venom (group III $sPLA_2$) enzymes were used as sources of $sPLA_2$. Enzymes were diluted in 10 μL of 100 mM Tris-HCl/1 mM $CaCl_2$ buffer, pH 7.5, and preincubated at 37 °C for 5 min with test compound or vehicle in a final volume of 250 μL. Incubation proceeded for 15 min in the presence of 20 μL of [^{3}H]oleic-*E. coli* membranes and was terminated by addition of 100 μL of ice-cold 0.25% bovine serum albumin (BSA) solution in saline to a final concentration of 0.07% (w/v). After centrifugation at 2500*g* for 10 min at 4 °C, the radioactivity in the supernatants was determined by liquid scintillation counting.

Western Blot Assay of COX-2 and mPGES-1. Cellular lysates from both RAW 264.7 (murine macrophages, 1.5×10^6 cells/mL) and THP-1 (human monocytic cell line, 1×10^6 cells/mL) incubated for 18 h with LPS (1 μg/mL) were obtained with lysis buffer A [10 mM *N*-(2-hydroxyethyl)piperazine-*N*′-ethanesulfonic acid (HEPES), pH 8.0, 1 mM ethylenediaminetetraacetic acid (EDTA), 1 mM ethylene glycol bis(β-aminoethyl ether)-*N*,*N*,*N*′,*N*′-tetraacetic acid (EGTA), 10 mM KCl, 1 mM dithiothreitol, 5 mM NaF, 1 mM Na_3VO_4, 10 mM Na_2MoO_4, 1 μg/mL leupeptin, 0.1 μg/mL aprotinin, and 0.5 mM phenylmethanesulfonyl fluoride). Following centrifugation (10000*g*, 15 min, 4 °C), supernatant protein was determined by the Bradford method with bovine serum albumin (BSA) as standard. COX-2 or mPGES-1 protein expression was studied in the total fraction or microsomal fraction, respectively. Equal amounts of protein (20 μg for COX-2 or 25 μg for mPGES-1 for RAW 264.7 cells; 30 μg for COX-2 or 100 μg for mPGES-1 for THP-1 cells), were subjected to SDS−15% PAGE and transferred onto poly(vinylidene difluoride) membranes for 90 min at 125 mA. Membranes were blocked in PBS (0.02 M, pH 7.0) Tween 20 (0.1%), containing 3% (w/v) nonfat milk and incubated with specific polyclonal antibody against COX-2 (1/1000 for RAW 264.7 cells and 1/200 for THP-1 cells) or mPGES-1 (1/200). Finally, membranes were incubated with peroxidase-conjugated goat anti-rabbit IgG (1/10 000). The immunoreactive bands were visualized by an enhanced chemiluminescence system (Amersham Biosciences, Barcelona, Spain).

Electrophoretic Mobility Shift Assay (EMSA). RAW 264.7 murine macrophages (1.5×10^6 cells/well) in 6-well plates were preincubated with different concentrations of tested compounds for 30 min and then stimulated with LPS (1 μg/mL) for 1 h. Nuclear extracts were prepared as described.[37] Cells were washed twice with ice-cold phosphate-buffered saline and then treated with 0.2 mL of buffer A for 15 min, followed by addition of Nonidet P-40 (0.5% w/v). The tubes were vortexed for 15 s, and nuclei were sedimented by centrifugation at 8000*g* for 30 s at 4 °C. Aliquots of the supernatant were stored at −80 °C (cytoplasmic extract), and the nuclear pellet was resuspended in 50 μL of buffer A supplemented with 0.4 M NaCl. After centrifugation at 13000*g* for 30 min at 4 °C, aliquots of the supernatant (nuclear extract) were stored at −80 °C. Protein was determined by the DC Bio-Rad protein reagent (Richmond, CA). Double-stranded oligonucleotides containing the consensus NF-κB (Promega Corp., Madison, WI) were end-labeled by use of T4 polynucleotide kinase (Amersham Biosciences, Barcelona, Spain) and [γ-^{32}P]ATP, followed by purification on G-25 microcolumns (Amersham Biosciences, Barcelona, Spain). Incubations were performed on ice with 6 μg of nuclear extract, 100 000 cpm of labeled probe, 2 μg of poly(dI-dC), 5% (v/v) glycerol, 1 mM EDTA, 5 mM $MgCl_2$, 1 mM dithiothreitol, 100 mM NaCl, and 10 mM Tris-HCl buffer (pH 8.0) for 15 min. Complexes were analyzed by nondenaturing 6% polyacrylamide gel electrophoresis in 45 mM Tris−borate buffer (pH 8.3) containing 1 mM EDTA, followed by autoradiography of the dried gel.

Culture of Murine Macrophage RAW 264.7 and Human Monocytic THP-1 Cell Lines. The mouse macrophage cell line RAW 264.7 (Cell Collection, Department of Animal Cell Culture, CSIC, Madrid, Spain) was cultured in Dulbecco's modified Eagle's medium (DMEM) containing 2 mM L-glutamine, 100 units/mL penicillin, 100 μg/mL streptomycin, and 10% fetal bovine serum. Cultures were maintained at 37 °C in a 5% CO_2 (air:CO_2 95:5) humidified incubator. Cells were resuspended at a concentration of 1.5×10^6 cells/mL. The human monocytic cell line THP-1 (American Type Culture, ATCC) was cultured in Roswell Park Memorial Insitute (RPMI) medium containing 2 mM L-glutamine, 100 units/mL penicillin, 100 μg/mL streptomycin, and 10% fetal bovine serum. Cultures were maintained at 37 °C in a 5% CO_2 (air:CO_2 95:5) humidified incubator. Cells were resuspended at a concentration of 1×10^6 cells/mL.

PGE_2 Production in RAW 264.7 Macrophages. RAW 264.7 macrophages (1.5×10^6 cells/mL) were co-incubated in 96-well culture plates (200 μL) with 1 μg/mL *Escherichia coli* [serotype 0111:B4] lipopolysaccharide (LPS) at 37 °C for 20 h in the presence of test compounds or vehicle. PGE_2 levels were determined in culture supernatants by radioimmunoassay.[38] The mitochondrial-dependent reduction of 3-(4,5-dimethylthiazol-2-yl)-2,5-diphenyltetrazolium bromide (MTT) to formazan[39] was used to assess the possible cytotoxic effects of compounds.

Mouse Air Pouch Model. All studies were performed in accordance with international regulations for the handling and use of laboratory animals. The protocols were approved by the institutional Animal Care and Use Committee. Air pouch was produce in female Swiss mice (25−30 g) as previously described.[40] Six days after the initial air injection, 1 mL of sterile saline or 1 mL of 1% (w/v) zymosan in saline was injected into the air pouch. Compound **4e** and dexamethasone were administered intrapouch at the same time as zymosan. After 24 h, the animals were killed by cervical dislocation and the exudate in the pouch was collected with 1 mL of saline. The cell pellets from air pouches were used to determine COX-2, mPGES-1, and β-actin by Western analysis as described above.

Statistical Analysis. The results are presented as mean ± SEM; *n* represents the number of experiments. Inhibitory concentration 50% (IC_{50}) values were calculated from at least four significant concentrations ($n = 6$). The level of statistical significance was determined by analysis of variance (ANOVA) followed by Dunnett's *t*-test for multiple comparisons. Significance was assumed at a *p* value of 0.05 or less.

Acknowledgment. We are grateful to Dr. Maria Chiara Monti for her contribution in the design of the compounds through the LUDI approach. Financial support by the University of Salerno and by MIUR (Rome) through the PRIN-2003 program is gratefully acknowledged. We also acknowledge the use of the instrumental (NMR and MS) facilities of the "Centro di Competenza in Diagnostica e Farmaceutica Molecolari" supported by Regione Campania (Italy) through POR funds. M.D.G. was the recipient of a research fellowship from the FPU program (AP 20041633) of the Spanish Ministerio de Educación y Ciencia. This work was supported in part by Grant FIS PI051659 from the Spanish Instituto de Salud Carlos III and by Grant UV-AE-20060243 from the University of Valencia.

Supporting Information Available: List of purity data (HPLC chromatograms) for target compounds. This material is available free of charge via the Internet at http://pubs.acs.org.

References

(1) Randazzo, A.; Debitus, C.; Minale, L.; García-Pastor, P.; Alcaraz, M. J.; Payá, M.; Gomez-Paloma, L. Petrosaspongiolides M−R: new potent and selective phospholipase A_2 inhibitors from new Caledonian marine sponge *Petrosaspongia nigra*. *J. Nat. Prod.* **1998**, *61*, 571−575.

(2) García, Pastor, P.; Randazzo, A.; Gomez-Paloma, L.; Alcaraz, M. J.; Payá, M. Effects of petrosaspongiolide M, a novel phospholipase A_2 inhibitor, on acute and chronic inflammation. *J. Pharmacol. Exp. Ther.* **1999**, *289*, 166−172.

(3) Posadas, I.; Terencio, M. C.; Randazzo, A.; Gómez-Paloma, L.; Payá, M.; Alcaraz, M. J. Inhibition of NF-κB signaling pathway mediates the anti-inflammatory effects of petrosaspongiolide M. *Biochem. Pharmacol*. **2003**, *65*, 887−895.

(4) (a) Dal Piaz, F.; Casapullo, A.; Randazzo, A.; Riccio, R.; Pucci, P.; Gennaro, M.; Gomez Paloma, L. Molecular basis of phospholipase A_2 inhibition by petrosaspongiolide M. *ChemBioChem*. **2002**, *3*, 664−671. (b) Monti, M. C.; Casapullo, A.; Riccio, R.; Gomez-Paloma, L. Further insights on the structural aspects of PLA_2 inhibition by γ-hydroxybutenolide-containing natural products: a comparative study on petrosaspongiolides M−R. *Bioorg. Med. Chem.* **2004**, *12*, 1467−74.

(5) (a) De Silva, E. D.; Scheuer, P. J. Manoalide, an antibiotic sesterterpenoid from the marine sponge *Luffariella variabilis* (Polejaeff). *Tetrahedron Lett.* **1980**, *21*, 1611−1614. (b) Potts, B. C. M.; Faulkner, D. J. Phospholipase A_2 inhibitors from marine organisms. *J. Nat. Prod.* **1992**, *55*, 1701−1717. (c) Potts, B. C. M.; Faulkner, D. J.; De Carvalho, M. S.; Jacobs, R. S. Chemical mechanism of inactivation of bee venom phospholipase A_2 by the marine natural products manoalide, luffariellolide, and scalaradial. *J. Am. Chem. Soc.* **1992**, *114*, 5093−5100.

(6) (a) De Rosa, S.; Crispino, A.; De Giulio, A.; Iodice, C. Cacospongionolide B, a new sesterterpene from the sponge *Fasciospongia cavernosa*. *J. Nat. Prod.* **1995**, *58*, 1776−1780. (b) Soriente, A.; Crispino, A.; De Rosa, M.; De Rosa, S.; Scettri, A.; Scognamiglio, G.; Villano, R.; Sodano, G. Stereochemistry of antiinflammatory marine sesterterpenes. *Eur. J. Org. Chem.* **2000**, *6*, 947−953. (c) Garcia Pastor, P.; De Rosa, S.; De Giulio, A.; Payá, M.; Alcaraz, M. J. Modulation of acute and chronic inflammatory processes by cacospongionolide B, a novel inhibitor of human synovial phospholipase A_2. *Br. J. Pharmacol.* **1999**, *126*, 301−311.

(7) (a) Gunasekera, S. P.; McCarthy, P. J.; Kelly-Borges, M.; Lobkovsky, E.; Clardy, J. Dysidiolide: A novel protein phosphatase inhibitor from the Caribbean sponge *Dysidea etheria* de Laubenfels. *J. Am. Chem. Soc.* **1996**, *118*, 8759−8760. (b) Takahashi, M.; Dodo, K.; Sugimoto, Y.; Aoyagi, Y.; Yamada, Y.; Hashimoto, Y.; Shirai, R. Synthesis of the novel analogues of dysidiolide and their structure−activity relationship. *Bioorg. Med. Chem. Lett.* **2000**, *10*, 2571−2574.

(8) Kernan, M. R.; Faulkner, D. J.; Parkanyi, L.; Clardy, J.; de Carvalho, M. S.; Jacobs, R. Luffolide, a novel anti-inflammatory terpene form the sponge, *Luffariella* sp. *Experientia* **1989**, *45*, 388−390.

(9) (a) Bohm, H. J. Current computational tools for *de novo* ligand design. *Curr. Opin. Biotechnol.* **1996**, *7*, 433−436. (b) Bohm, H. J. Site-directed structure generation by fragment-joining. *Perspect. Drug Discovery Des.* **1995**, *3*, 21−33. (c) Bohm, H. J. On the use of LUDI to search the find chemicals directory for ligands of protein of known three-dimensional structure. *J. Comput. Aided Mol. Des.* **1994**, *8*, 623−632.

(10) Bellina, F.; Rossi, R. Mucochloric and mucobromic acids: inexpensive, highly functionalised starting materials for the selective synthesis of variously substituted 2(5*H*)-furanone derivatives, sulfur- or nitrogen-containing heterocycles and stereodefined acyclic unsaturated dihalogenated compounds. *Curr. Org. Chem.* **2004**, *12*, 1089−1103

(11) (a) Miyaura, N.; Suzuki, A. Palladium-catalyzed cross-coupling reactions of organoboron compounds. *Chem. Rev.* **1995**, *95*, 2457−2483. (b) Wallow, T. I.; Novak, B. M. Highly efficient and accelerated Suzuki aryl couplings mediated by phosphine-free palladium sources. *J. Org. Chem.* **1994**, *59*, 5034−5037.

(12) Corey, E. J.; Gras, J.-L.; Ulrich, P. A new general method for protection of the hydroxyl function. *Tetrahedron Lett.* **1976**, *11*, 809−812.

(13) (a) Soriente, A.; De Rosa, M.; Scettri, A.; Sodano, G.; Terencio, M. C.; Payá, M.; Alcaraz, M. J. Manoalide. *Curr. Med. Chem.* **1999**, *6*, 415−431. (b) Gomez-Paloma, L.; Monti, M. C.; Terracciano, S.; Casapullo, A.; Riccio, R. Chemistry and biology of anti-inflammatory marine natural products. Phospholipase A_2 inhibitors. *Curr. Org. Chem.* **2005**, *9*, 1419−1427.

(14) Masuda, S.; Murakami, M.; Komiyana, K.; Ishihara, M.; Ishikawa, Y.; Ishii, T.; Kudo, I. Various secretory phospholipase A_2 enzymes are expressed in rheumatoid arthritis and augment prostaglandin production in cultured synovial cells. *FEBS J.* **2005**, *272*, 655−672.

(15) Wu, A.; Hinds, C. J.; Thiemermann, C. High-density lipoproteins in sepsis and septic shock: metabolism, actions, and therapeutic applications. *Shock* **2004**, *21*, 210−221.

(16) Haas, U.; Podda, M.; Behne, M.; Gurrieri, S.; Alonso, A.; Furstenberger, G.; Pfeilschifter, J.; Lambeau, G.; Gelb, M. H.; Kaszkin, M. Characterization and differentiation-dependent regulation of secreted phospholipases A_2 in human keratinocytes and in healthy and psoriatic human skin. *J. Invest. Dermatol*. **2005**, *124*, 204−211.

(17) Offer, S.; Yedgar, S.; Schwob, O.; Krimsky, M.; Bibi, H.; Eliraz, A.; Madar, Z.; Shoseyov, D. Negative feedback between secretory and cytosolic phospholipase A_2 and their opposing roles in ovoalbumin-induced bronchoconstriction in rats. *Am. J. Physiol.: Lung Cell Mol. Physiol*. **2005**, *288*, 523−529.

(18) Balsinde, J.; Balboa, M. A.; Insel, P. A.; Dennis, E. A. Regulation and inhibition of phospholipase A_2. *Annu. Rev. Pharmacol. Toxicol.* **1999**, *39*, 175−189.

(19) Westman, M.; Korotkova, M.; af Klint, E.; Stark, A.; Audoly, L. P.; Klareskog, L.; Ulfgren, A. K.; Jakobsson, P. J. Expression of microsomal prostaglandin E synthase 1 in rheumatoid arthritis synovium. *Arthritis Rheum.* **2004**, *50*, 1774−1780.

(20) Nakano, H.; Shindo, M.; Sakon, S.; Nishinaka, S.; Mihara, M.; Yagita, H.; Okumura, K. Differential regulation of IκB kinase alpha and beta by two upstream kinases, NF-κB-inducing kinase and mitogen-activated protein kinase/ERK kinase kinase-1. *Proc. Natl. Acad. Sci. U.S.A.* **1998**, *95*, 3537−3542.

(21) Mendez, M.; La Pointe, M. C. PPARgamma inhibition of cyclooxygenase-2, PGE_2 synthase, and inducible nitric oxide synthase in cardiac myocytes. *Hypertension* **2003**, *42*, 844−850.

(22) Subbaramaiah, K.; Yoshimatsu, K.; Scherl, E.; Das, K. M.; Glazier, K. D.; Golijanin, D.; Soslow, R. A.; Tanabe, T.; Naraba, H.; Dannenberg, A. J. Microsomal prostaglandin E synthase-1 is overexpressed in inflammatory bowel disease. Evidence for involvement of the transcription factor Egr-1. *J. Biol. Chem.* **2004**, *279*, 12647−12658.

(23) Fahmi, H. mPGES-1 as a novel target for arthritis. *Curr. Opin. Rheumatol.* **2004**, *16*, 623−627.

(24) Lawrence, T.; Willoughby, D. A.; Gilroy, D. W. Anti-inflammatory lipid mediators and insights into the resolution of inflammation. *Nat. Rev. Immunol.* **2002**, *2*, 787−795.

(25) Narumiya, S.; FitzGerald, G. A. Genetic and pharmacological analysis of prostanoid receptor function. *J. Clin. Invest.* **2001**, *108*, 25−30.

(26) Serhan, C. N.; Levy, B. Success of prostaglandin E_2 in structure−function is a challenge for structure-based therapeutics. *Proc. Natl. Acad. Sci. U.S.A.* **2003**, *100*, 8609−8611.

(27) Murakami, M.; Kudo, I. Recent advances in molecular biology and physiology of the prostaglandin E_2-biosynthetic pathway. *Prog. Lipid Res.* **2004**, *43*, 3−35.

(28) Bomalaski, J. S.; Clark, M. A. Phospholipase A_2 and arthritis. *Arthritis Rheum.* **1993**, *36*, 190−198.

(29) Crofford, L. J. Clinical experience with specific COX-2 inhibitors in arthritis. *Curr. Pharm. Des.* **2000**, *6*, 1725−1736.

(30) Murakami, M.; Nakashima, K.; Kamei, D.; Masuda, S.; Ishikawa, Y.; Ishii, T.; Ohmiya, Y.; Watanabe, K.; Kudo, I. Cellular prostaglandin E_2 production by membrane-bound prostaglandin E synthase-2 via both cyclooxygenases-1 and 2. *J. Biol. Chem.* **2003**, *278*, 37937−37947.

(31) Jakobsson, P. J.; Thoren, S.; Morgenstern, R.; Samuelsson, B. Identification of human prostaglandin E synthase: a microsomal glutathione-dependent inducible enzyme, constituting a potential novel drug target. *Proc. Natl. Acad. Sci. U.S.A.* **1999**, *96*, 7220−7225.

(32) Thoren, S.; Weinander, R.; Saha, S.; Jegerschold, C.; Petterson, P. L.; Samuelsson, B.; Hebert, H.; Hamberg, M.; Morgenstern, R.; Jakobsson, P. J. Human microsomal prostaglandin E synthase-1: purification, functional characterization and projection structure determination. *J. Biol. Chem.* **2003**, *278*, 22199−22209.

(33) Stichtenoth, D. O.; Thoren, S.; Bian, H.; Peters-Golden, M.; Jakobsson, P. J.; Crofford, L. J. Microsomal prostaglandin E synthase is regulated by proinflammatory cytokines and glucocorticoids in primary rheumatoid synovial cells. *J. Immunol.* **2001**, *167*, 469−474.

(34) Korotkova, M.; Westman, M.; Gheorghe, KR.; af Klint, E.; Trollmo, C.; Ulfgren, A. K.; Klareskog, L.; Jakobsson, P. J. Effects of antirheumatic treatments on the prostaglandin E_2 biosynthetic pathway. *Arthritis Rheum.* **2005**, *52*, 3439−3447.

(35) Franson, R.; Patriarca, P.; Elsbach, P. Phospholipid metabolism by phagocytic cells: Phospholipase A_2 associated with rabbit polymorphonuclear leukocyte granules. *J. Lipid. Res.* **1974**, *15*, 380−388.

(36) Payá, M.; Terencio, M. C.; Ferrándiz, M. L.; Alcaraz, M. J. Involvement of secretory phospholipase A_2 activity in the zymosan rat air pouch model of inflammation. *Br. J. Pharmacol.* **1996**, *117*, 1773−1779.

(37) López-Collazo, E.; Hortelano, S.; Rojas, A.; Boscá, L. Triggering of peritoneal macrophages with IFN-α/β attenuates the expression of inducible nitric oxide synthase through a decrease in NF-κB activation. *J. Immunol.* **1998**, *160*, 2889−2995.

(38) Hoult, J. R.; Moroney, M. A.; Payá, M. Actions of flavonoids and coumarins on lipoxygenase and cyclooxygenase. *Methods Enzymol.* **1994**, *234*, 443−454.

(39) Gross, S. S.; Levi, R. Tetrahydrobiopterin synthesis: An absolute requirement for cytokine-induced nitric oxide generation by vascular smooth muscle. *J. Biol. Chem.* **1992**, *267*, 25722−25729.

(40) Posadas, I.; Terencio, M. C.; Guillén, I.; Ferrándiz, M. L.; Coloma, J.; Payá, M.; Alcaraz, M. Co-regulation between cyclo-oxygenase-2 and inducible nitric oxide synthase expression in the time-course of murine inflammation. *Naunyn-Schmiedeberg's Arch. Pharmacol.* **2000**, *361*, 98−106.

JM0700823